biologia plantarum
an international journal for experimental botany

BIOLOGIA PLANTARUM (2021) 65: 283-296 DOI: 10.32615/bp.2021.035

Identification of three gene families coordinating the conversion between fructose-6-phosphate and fructose-1,6-bisphosphate in wheat

C.M. YU[1,*], Y.C. KE[1], K.P. ZHANG[2], M. YAN[1], H.R. JIN[1], Y.H. CHEN[1], J. ZHANG[1]

[1] *School of Life Sciences, Nantong University, Nantong, 226019, Jiangsu Province, P.R. China*
[2] *State Key Laboratory of Plant Cell and Chromosome Engineering, Institute of Genetics and Developmental Biology, Chinese Academy of Science, Beijing, 100101, P.R. China*

[*]Corresponding author: E-mail: ychmei@ntu.edu.cn

Abstract

Saccharides are a direct energy source for most organisms and the primary components in grains of common wheat (*Triticum aestivum* L., 2n = 6x = 42, AABBDD). However, genes involved in the metabolism of primary saccharides such as glucose and fructose have not been fully characterized in wheat, which limits our understanding of how these genes influence wheat growth. In this study, genes coding ATP-dependent phosphofructokinase (PFK), fructose-1,6-bisphosphatase (FBP), and pyrophosphate-dependent fructose-6-phosphate 1-phosphotransferase (PFP), which participate in the conversion between fructose 6-phosphate (F-6-P) and fructose 1,6-bisphosphate (F-1,6-P_2), were identified at the genome-wide level. A total of 24, 13, and 12 genes were found encoding *TaPFK*, *TaFBP*, and *TaPFP,* respectively. All predicted peptides of these genes exhibited conserved substrate-binding domain, suggesting they are active enzymes *in vivo*. Transcriptome data ranked the gene levels as follows: *TacyFBP*-1 > *TacpFBP*-1 > *TaPFPα*-2 ≈ *TaPFPβ* >> *TaPFK*-1 ≈ *TaPFK*-5 >> all remaining genes at different developmental stages of wheat. In the three *tapfp-a, b,* and *d* knockout lines, there was a decrease in the plant height, anther length, and thousand-grain mass, while the percentage of abnormal pollen increased compared to that of wild type cv. Huapei3 (HP3). During germination, *tapfpβ-a* exhibited a lower germination rate, shorter coleoptile and primary root length, and higher fructose content than HP3, *tapfpβ-b*, and *tapfpβ-d* lines. Expressions were ranked as follows: *TaPFK*-5 ≈ *TaPFPα*-2 >> *TaPFPα*-1 ≈ *TaPFPβ* > *TacyFBP*-1 ≈ *TaPFK*-7, 9 in HP3. All these genes were downregulated during the 24 - 96 h germinating process in three mutant lines. Collectively, main *TaPFK*, *TaFBP,* and *TaPFP* members cooperated during wheat growth, while *TaPFPβ* knockout decreased wheat vitality. Results from this study can aid more systematic studies of the physiological and molecular functions of *TaPFK*, *TaFBP,* and *TaPFP*.

Keywords: ATP-dependent phosphofructokinase, fructose-1,6-bisphosphatase, germination, pyrophosphate-dependent fructose-6-phosphate 1-phosphotransferase, transcriptome, *Triticum aestivum.*

Introduction

In crop seeds, such as wheat, rice, and maize, activated glucose-1-phosphate (G-1-P) is a substrate for sucrose and starch synthesis (Pfister and Zeeman 2016). During germination of the crop seeds, starch breaks down

Received 6 February 2021, *last revision* 2 June 2021, *accepted* 9 June 2021.
Abbreviations: F-1,6-P_2 - fructose-1,6-bisphosphate; F-2,6-P_2 - fructose-2,6-bisphosphate; F-6-P - fructose-6-phosphate; FBP - fructose-1,6-bisphosphatase; G-1-P - glucose-1-phosphate; HP3 - Huapei3; Mr - molecular mass; PAGE - polyacrylamide gel electrophoresis; PFK - ATP-dependent phosphofructokinase; PFP - pyrophosphate-dependent fructose-6-phosphate 1-phosphotransferase; pI - isoelectric point; PPP - pentose phosphate pathway; SBP -sedoheptulose-1,7-bisphosphatase; TCA - tricarboxylic acid; TGM - thousand-grain mass; TPM - transcripts per million.
Acknowledgements: This research was supported by the National Program on Key Basic Research Project (2016YFD0100500). We thank Z.Y. Mao for assistance in propagating the wheat mutant population in the field station and all colleagues at the Lab Center of the School of Life Sciences of Nantong University for assistance in the use of instruments.
*Conflict of interest***:** The authors declare that they have no conflict of interest.

to G-1-P to afford ATP, NADPH, and intermediate metabolites through glycolysis, the tricarboxylic acid (TCA) cycle, and pentose phosphate pathway (PPP) (Fig. 1 Suppl.) (Fernie *et al*. 2004). In the glycolysis and gluconeogenesis pathway, G-1-P is converted to fructose-6-phosphate (F-6-P) through two reversible steps, while the conversion between F-6-P and fructose-1,6-bisphosphate (F-1,6-P_2) is irreversibly catalyzed by ATP-depended phosphofructokinase (PFK) in the glycolysis pathway and fructose-1,6-bisphosphatase (FBP) in gluconeogenesis pathway, respectively (Fig. 1 Suppl.), or reversibly converted by a pyrophosphate-dependent fructose-6-phosphate 1-phosphotransferase (PFP) (Fig. 1 Suppl.) (Ap Rees *et al*. 1985, Montavon and Kruger 1992, Plaxton and Podestá 2007). Although previous studies have investigated PFK, FBP, and PFP enzymes individually in plants, limited studies have investigated their cooperation during plant growth.

Studies on *Arabidopsis thaliana*, *Oryza sativa*, *Saccharum* species, *Spinacia oleracea*, and *Pyrus bretschneideri* have shown that isoforms of PFKs are encoded by a small gene family comprising three sub-class (*PFK-A*, *-B,* and *-C,* respectively) (Knowles 1990, Winkler *et al*. 2007, Mustroph *et al*. 2007, 2013, Zhu *et al*. 2013, Lü *et al*. 2019). Functional studies have shown that plant PFKs may be involved in several processes. For example, *OsPFK-Bs* are downregulated, while *OsPFK-Cs* are induced under anoxia stress (Mustroph *et al*. 2013). Transient transformation of plastid *PbPFK1* in pear fruits significantly increased fructose and sorbitol content (Lü *et al*. 2019). Furthermore, *PFK* members in a plant are differently expressed; for example, 3 out of 10 *Saccharum ScPFKs* are highly expressed in sugarcane (Zhu *et al.* 2013).

FBP dephosphorylates F-1,6-P_2 (Fig. 1 Suppl.). Plants have two isoforms of FBP, namely cytosolic FBP (cyFBP) and chloroplast FBP (cpFBP), which exhibit approximately 50 % sequence identity and are derived from a gene duplication event during early eukaryotic evolution (Martin *et al.* 1996, Jiang *et al*. 2012, Gutle *et al*. 2016). The cyFBP is primarily involved in gluconeogenesis and sucrose biosynthesis, whereas cpFBP participates in photosynthesis (Rojas-Gonzalez *et al*. 2015). The disruption of *OscyFBP1* hinders growth due to a reduction in photosynthetic rate and chlorophyll content (Lee *et al*. 2008). Loss of *AtcyFBP* has no significant effect on the phenotype, but increases chloroplast starch content, whereas *AtcpFBP* knockout plants exhibit a smaller rosette size, increased superoxide dismutase activity, lower photosynthesis rate, soluble sugar content, and starch accumulation. *AtcpFBP* and *AtcyFBP* double mutants exhibit a dwarf phenotype (Rojas-Gonzalez *et al*. 2015, Soto-Suarez *et al*. 2016). The above data from rice and *Arabidopsis* suggested cooperation between cy- and cpFBP.

Among the three enzymes (PFK, FBP, and PFP), PFP has been extensively studied. PFP exists as a heterotetramer with two regulatory alpha-subunits (FPFα) and two catalytic beta-subunits (FPFβ), and its activity is tightly regulated by fructose-2,6-bisphosphate (F-2,6-P_2) (Tripodi and Podesta 1997, Fernie *et al*. 2001, 2002, Nielsen *et al*. 2004). FPFα is encoded by several genes, whereas FPFβ is encoded by a single gene in monocots (Mustroph *et al*. 2013, Lü *et al*. 2019). Functional studies have illustrated that PFP is not only involved in glycolysis/gluconeogenesis, but also in pyrophosphate (PPi) generation for hydrogen proton pumping in tonoplast and stress responses to N and P limitations and hypoxia (Costa dos Santos *et al*. 2003, Basson *et al*. 2011, Lim *et al*. 2013, Mustroph *et al*. 2013, Duan *et al*. 2016). *Arabidopsis PFP*-knockout plants have growth retardation phenotype (Lim *et al*. 2009), while frame-shift mutation of *OsPFPβ* causes opaque, brittle, and floury grains, but no visible abnormal phenotype during the seedling and tilling stages (Duan *et al*. 2016, Chen *et al*. 2020a). These results indicate that PFP may function differently in different plants. Whether disturbing one of these three genes' expression affects the other two remains to be determined.

Common wheat is a hexaploid species (2n = 6x = 42, AABBDD) derived from three diploid progenitors in two rounds of natural hybridization (Marcussen *et al*. 2014), and most of its genes have three homoeologs. As the second largest crop, wheat yield is important for global food security (Senapati and Semenov 2020, Shew *et al*. 2020). Therefore, to determine the relationship between carbon metabolism and wheat yield, we identified *TaPFK*, *TaPFP*, and *TaFBP* genes in the wheat genome, determined their expression in different tissues using publicly available RNA-seq data to characterize the main functional members during different developmental stages (Brenchley *et al*. 2012, Jia *et al*. 2013, Ling *et al*. 2013, International Wheat Genome Sequencing Consortium 2014, 2018). To better understand the function of *TaPFP* and investigate the cooperation between *PFP*, *PFK,* and *FBP* genes in wheat, phenotype [plant height, thousand-grain mass (TGM), anther morphology, pollen fertility] of the three *tapfpβ* homoeologous gene knock-out mutant lines was observed, *TaPFK*, *TaPFP*, and *TaFBP* gene expression during the germination process were also determined in this study.

Materials and methods

Plants and reagents: *Triticum aestivum* L. cv. Huapei 3 (HP3) and a fast neutron-induced mutant population of the HP3 genetic background (4 500 lines from 8 000 seeds treated with 1×10^{11} n.cm^{-2} fast neutrons, obtained from the Institute of Genetic and Developmental Biology, Chinese Academy of Sciences) were used in this study. Common wheat cultivar Chinese Spring (CS) and its null-tetrasomic (NT) lines were used as references in genotype screening. Twenty seeds of all lines were sown in one row (100 cm) in the field (Plant Field Station of the School of Life Sciences of Nantong University, E:120.62°, N:32.13°) during the 2017 - 2019 growth season (row spacing 25 cm, mid-November to May the next year).

Primers used for *PFP* mutant screening and quantitative reverse transcription (RT-qPCR) analysis are listed in Table 1 Suppl. Oligo primers were synthesized by *General*

Biosystems (Chuzhou, Anhui, China). PCR reagents, DNA polymerase (*ExTaq*), and DNA markers (50-bp ladder, DL 5000) were purchased from *TaKaRa* (Daliang, Liaoning, China). DNA was isolated using a plant DNA isolation kit (*Tangen*, Beijing, China). RNA was extracted using a plant universal RNA isolation kit (*TaKaRa*). The cDNA was generated using a first-strand cDNA synthesis kit from *TaKaRa*. All kits were used according to the manufacturer's instructions. All other chemical reagents (analytical purity) were purchased from *SinoPharm* (Nanjing, China) or *Amresco* (Houston, TX, USA).

Phylogenetic analysis and prediction of protein features: The latest versions of the genome sequences of *A. thaliana*, *Oryza sativa*, *Aegilops tauschii* (2n = 14, DD), and wheat (*Triticum urartu*, 2n = 14, AA, *Triticum dicoccoides*, 2n = 24, AABB, and *T. aestivum*, 2n = 42, AABBDD) were downloaded from the *Ensemble* database (http://plants.ensembl.org/); and those of *Brachypodium distachyon* (Bd21) and *Hordeum vulgare* (2n = 14, HH) were downloaded from *Phytozome* (https://phytozome.jgi.doe.gov/pz/portal.html). Seed files of PFK (PF00365) and FBP (PF00136) domains were downloaded from the *Pfam* website (http://pfam.xfam.org/) and used to search the plant peptide databases mentioned above using *HMMER*. The e-value cut-off was 10^{-20} and *SMART* (http://smart.embl-heidelberg.de) and *CDD* (https://www.ncbi.nlm.nih.gov/cdd) were used to confirm the sequences obtained. Only one peptide sequence of every gene was kept for further phylogenetic and gene structural analysis, and sequences that were too long or too short were manually excluded. Multiple alignments of PFK, PFP, and FBP peptide sequences were generated using *ClustalW*, and phylogenic trees of PFK, PFP, and FBP were constructed using the neighbor-joining method with 1 000 bootstrap replicates in *MEGA7* (Saitou and Nei 1987, Kumar *et al*. 2016). Newick format files of phylogenic trees of *TaPFK*, *TaPFP*, and *TaFBP* genes were saved for further use. The isoelectric point (pI) and relative molecular mass (Mr) of proteins were predicted using the *ExPASy* web server (https://web.expasy.org/compute_pi/) and the sublocalization of these proteins was predicted on the website of *TargetP* (http://www.cbs.dtu.dk/services/TargetP/). Nomenclature of the *TaPFK, TaPFP,* and *TaFBP* was based on gene name of *Arabidopsis* and rice (Martin *et al.* 1996, Mustroph *et al.* 2007, 2013, Lee *et al.* 2008, Serrato *et al.* 2009, Jiang *et al.* 2012, Gutle *et al.* 2016).

Gene feature analyses: Conserved motifs in PFK, PFP, and FBP were analyzed using *MEME* (http://meme-suite.org), with parameter settings according to Lü *et al*. (2019): expected motif sites: zero or one per sequence; maximum number of motifs: 15; minimum motif width: 6; maximum motif width: 50; and maximum number of sites: 300. Results were exported in XML format. A figure combining the phylogenic tree, conserved motifs, and gene structure was generated by submitting gene IDs of *TaPFKs*, *TaPFKs*, and *TaPFPs* (Table 1), a phylogenetic tree file (*.Newick), a conserved motif file (*.xml), and the *Triticum_aestivum*. IWGSC.44.gff3 file to the graphics tools of *TBtools* (Chen *et al.* 2020b). The conserved motifs of TaPFK/PFPs were compared to *Escherichia coli* PFK (PDB1PFK) (Ronimus and Morgan 2001), while the *TaFBPs* were compared to the *AtFBPs* (Chueca *et al*. 2002, Serrato *et al*. 2009, Gutle *et al*. 2016).

Mining transcriptions through RNA-seq database: Expression data of all three gene families at different developmental stages of Chinese Spring (CS) were downloaded from the *Triticeae* Multi-omics Center (http://202.194.139.32/) according to Borrill *et al.* (2016). An expression heatmap was drawn using the *HeatMap* tool in TBtools (Chen *et al.* 2020b).

***TaPFPβ* mutant screening and phenotypic analysis**: In total, 4 500 lines of a fast neutron-induced mutant population of HP3 were subjected to genotype identification using a pair of conserved primers specific to three *TaPFP* genes (Table 1 Suppl.). PCR products were separated by 6 % undenatured polyacrylamide gel electrophoresis (PAGE) and visualized using silver staining according to Merril (1990). Gene-specific primers (Table 1 Suppl.) were designed to detect the expression of the three homologous genes in leaves, to verify the mutants.

Seeds of mutant lines were surface-sterilized once using 70 % (v/v) ethanol and 0.1 % (m/v) *Tween-20* for 10 min, washed with double-distilled water for at least five times, and germinated in Petri dishes (diameter 12 cm) on wet filter paper at 18 °C (night) and 22 °C (day) in the dark. At least 100 seeds and three repeats were used to analyze the germination rate. The lengths of primary roots and coleoptile were measured after 112 h of germination. Plant height was measured after full heading in the field during the growth season (n > 50, 2018 - 2019). The thousand-grain mass (TGM) was measured in three repeats after the seeds were dried to a constant mass.

Spikelets of HP3 and three mutant lines, 2 - 3 d before flowering, were fixed in formalin-aceto-alcohol solution (85 cm^3 of 95 % ethanol, 5 cm^3 of acetic acid, 5 cm^3 of formalin, 5 cm^3 of glycerol in a 100-cm^3 solution). Paraffin sections were prepared according to the methods described by Cao *et al*. (2012). Sections were observed and imaged under *Zeiss Axioscope* 1 microscope (*Oberkochen*, Germany). All data were collected from at least three biological repeats.

Pollen was collected during flowering and stained by iodine-potassium iodide solution (I_2-KI, 0.5 g iodine, and 1 g potassium iodide in 100 cm^3 ddH_2O) to observe the phenotypes.

Real-time qPCR analysis of *PFK*, *FBP*, and *PFP* expression during germination: Total RNA was extracted from the grain after 24 - 96 h of germination and used for first-strand cDNA synthesis. Gene-specific primers were designed for the three homologous genes (Table 1 Suppl.). An *ABI 7500* instrument with software version *2.3.1* (*Applied Biosystems*, Foster City, CA, USA) was used for qPCR analysis; wheat *26S rRNA* gene was used as an internal control (Ali-Benali *et al*. 2005). qPCR mixture composition and PCR conditions were as per

the manufacturer's instructions. Relative mRNA content was calculated using the $2^{-\Delta\Delta Ct}$ method for at least three technical and three biological repeats (pooled).

Soluble sugar detection: One gram of fresh endosperm collected at 24, 48, 72, and 96 h after germination was homogenized in 10 cm^3 of distilled water. The homogenates were transferred into 100-cm^3 flasks and incubated at 50 °C for 30 min. Then, they were filtered through a four-layer gauze and distilled water was added to a final volume of 50 cm^3. Sucrose, fructose, and glucose were detected by ion-exchange chromatography as described by Noggle and Zill (1952). At least three biological and technical repeats were included.

Data analysis: Data were illustrated using graphs with *SigmaPlot 9.0* and presented as the mean ± standard deviation (SD), which were calculated in *Excel*. Means were compared using Student's *t*-test in *SPSS17* (*IMB*, Armonk, USA). $P < 0.05$ was considered as significant.

Results and discussion

Genes containing PFK (PF00365) and FBP (PF00136) domains were searched in the genomes of *Arabidopsis*, rice, *Brachypodium*, barley, *T. urartu*, *Ae. tauschii*, *T. dicoccoides*, and *T. aestivum*. We found 49 genes encoding TaPFK, TaPFP, and TaFBP, and they were scattered over all 21 wheat chromosomes (Table 1).

In a phylogenetic tree of PFKs/PFPs constructed using the neighbor-joining method, PFKs and PFPs clearly formed separate clusters (Fig. 2 Suppl.). According to the evolutional analysis of *AtPFKs* and *OsPFKs*, the nomenclatures for *TaPFK* followed the *OsPFKs* (Mustroph *et al*. 2007, 2013) (Table 1, Fig. 2 Suppl.). Fig. 2 Suppl. shows the homologous relationships of *PFKs/PFPs* in grass species. Loss of gene members was found in the *PFK_A* and *PFP_ALPHA* sub-groups. Five members of *PFK_A* were found in rice and *Brachypodium*, whereas only four members were identified in barley, *T. urartu*, *Ae. tauschii*, *T. dicoccoides*, and *T. aestivum* (Table 1, Fig. 2 Suppl.**)**. This indicated that an event of gene loss happened after the divergence of the *Brachypodium*/*Triticeae* species. The phylogenic analysis also showed that one member of *PFP_ALPHA* was lost between the divergence of rice and the ancestor of *Brachypodium* and *Triticeae*, before the loss of the *PFK_A* member.

When using sedoheptulose-1,7-bisphosphatase (*SBP*) as an outgroup, *FBPs* in the phylogenic tree were clustered in four subgroups (Fig. 3 Suppl.), and nomenclature for *TaFBPs* was according to the *AtFBPs* and *OsFBPs* (Fig. 3 Suppl.) (Martin *et al.* 1996, Lee *et al*. 2008, Serrato *et al*. 2009, Jiang *et al*. 2012) (Table 1). Fig. 3 Suppl. shows that all grass species had two copies of cy*FBPs* and *cpFBPs*, whereas *Arabidopsis* only had one of each, indicating that a whole-genome duplication event happened after the divergence of *Arabidopsi*s and the grass ancestor. Furthermore, from the chromosome location of *cyFBP2-D1* and *-D2* (Table 1), it seemed that a tandem duplication took place, which may be due to template slipping during DNA replication (Wang *et al*. 2018). The four *cyFBP2-D* members (at di- and hexaploidy levels) clustered in two clades, with one clade more closely resembling *cyFBP2-A*, and the other being closer to *cyFBP2-B* (Table 1, Fig.2, Fig. 3 Suppl.). Hence the two *cyFBP2-D* copies originated from different progenitors and were orthologous and not paralogous genes.

Through the phylogenic relationships of *PFKs*, *PFPs*, and *FBPs* in eight plant genomes, whole-genome duplication and segmental loss or duplication shaped these genes in the grass genome (Fig. 2 Suppl. and Fig. 3 Suppl.). A previous study showed that wheat chromosomes 1 (w1) and 3 (w3) are orthologous to rice chromosomes 1 (r1) and 5 (r5) (Salse *et al*. 2008); based on synteny and gene orders, authors concluded that duplication of w1/w5 and r1/r5 arose by large segmental duplication during the evolution of the ancestor's genome. In this study, *TaPFKAs* and *TacyFBPs* located on w1 and w3 clustered together with their rice orthologs (Fig. 2 Suppl. and Fig. 3 Suppl.). In addition, copy numbers of the homoeologous genes in wheat showed good agreement with the ploidy levels, *e.g*., one, two, and three copies of *TaPFK-A5* in the di-, tetra-, and hexaploid species (Table 1, Fig. 2 Suppl.). Mirzaghaderi and Mason (2017) suggested three possible mechanisms underlying the evolution of allohexaploid wheat, including "inherited," "modified," and "induced" models. They suggested that all three mechanisms may be at work, and none of the mechanisms are entirely mutually exclusive. Based on our findings, we believe the "inherited" model may be more suitable to explain the phylogenetic relationships of *PFKs*, *PFPs*, and *FBPs* among the three wheat subgenomes and their progenitors, since the chromosome locations and gene copies did not vary in the wheat subgenomes (Tables 1, Fig. 2 Suppl. and Fig. 3 Suppl). The phylogenic relationship of the wheat PFK, FPF, and FBP, and other plants, found herein, can be used to compare the function among orthologs in a plant.

Most homoeologous TaPFK, TaPFP, and TaFBP proteins have similar peptide lengths, theoretical pI, Mr, sublocalization, and genetic exon-intron structure (Table 1, Figs. 1 and 2). However, the pIs of the homoeologous members, including TaPFK-6, TaPFK-8, and TacpFBP1, differed more than 0.5 pH unit. Interestingly, the pIs of seven PFKs (TaPFK-1, -2, -5, -6 -7, -8, and -10) and two cpFBPs (TacpFBP-1 and -2) differed more than 1 pH unit.

Analysis of the conserved motifs showed that all TaPFKs/PFPs have five conserved motifs, 1 - 4 and 9, which were organized in the same order (Fig. 1). When TaPFK/PFPs was aligned to *Escherichia coli* PFK (PDB1PFK) (Ronimus and Morgan 2001), the F-6-P binding sites were in motifs 1 - 4 and 9, and the binding site for ATP, which is the specific substrate for PFKs, was in motif 8 (Fig. 1). PFP forms a heterotetramer (α2β2), α3β3 heterohexamer, or α4β4 hetero-octamer in different plants (Theodorou and Plaxton 1996, Turner and Plaxton 2003, Muchut *et al.* 2019). Nine PFPα and three PFPβs members were found in wheat (Table 1, Fig. 1). However, how α and β subunits organize into a whole enzyme in wheat requires further research. More interestingly, how the nine α subunits and

Table 1. Characteristics of TaPFKs, TaPFPs, and TaFBPs. Traes - *Triticum aestivum*; CS - Chinese Spring; a.a. - number of amino acids; NE - number of exons (UTRs excluded). *Grey shade* indicates a pI difference larger than 0.5 pH units among the three homoeologous proteins. Cy - cytoplasmic; Cp - chloroplast. A, B, and D in the gene ID stands for the subgenome. The number before subgenome is the group.

Subclass	*T. aestivum*	Gene name	Length of peptide [a.a.]	pI / Mr [kDa]	Sublocalization	NE
PFK_A	TraesCS3A02G107600	*TaPFK-A1*	535	7.21 / 58.212	Cy	11
	TraesCS3B02G126400	*TaPFK-B1*	535	7.21 / 58.055	Cy	11
	TraesCS3D02G109600	*TaPFK-D1*	535	7.21 / 57.998	Cy	11
	TraesCS3A02G277700	*TaPFK-A2*	609	5.85 / 66.620	Cy	15
	TraesCS3B02G311900	*TaPFK-B2*	608	5.97 / 66.606	Cy	15
	TraesCS3D02G278000	*TaPFK-D2*	609	5.88 / 66.672	Cy	15
	TraesCS1A02G344000	*TaPFK-A5*	569	6.61 / 62.242	Cy	14
	TraesCS1B02G357000	*TaPFK-B5*	566	6.61 / 62.044	Cy	14
	TraesCS1D02G346200	*TaPFK-D5*	569	6.58 / 62.287	Cy	14
	TraesCS7A02G106800	*TaPFK-A6*	494	7.21 / 53.844	Cy	13
	TraesCS7B02G005500	*TaPFK-B6*	488	6.68 / 53.466	Cy	13
	TraesCS7D02G101300	*TaPFK-D6*	494	6.37 / 53.902	Cy	13
PFK_B	TraesCS2A02G331700	*TaPFK-A9*	469	6.05 / 50.735	Cy	2
	TraesCS2B02G350500	*TaPFK-B9*	469	5.97 / 50.796	Cy	2
	TraesCS2D02G331200	*TaPFK-D9*	469	6.15 / 50.732	Cy	2
PFK_C	TraesCS7A02G088100	*TaPFK-A7*	529	8.68 / 58.117	Cy/Cp	13
	TraesCS4A02G387000	*TaPFK-B7*	529	8.73 / 58.093	Cy/Cp	13
	TraesCS7D02G083200	*TaPFK-D7*	529	8.60 / 58.199	Cy/Cp	13
	TraesCS5A02G226600	*TaPFK-A8*	530	7.59 / 58.097	Cy/Cp	13
	TraesCS5B02G225200	*TaPFK-B8*	530	7.28 / 58.123	Cy/Cp	13
	TraesCS5D02G234000	*TaPFK-D8*	530	7.05 / 57.840	Cy/Cp	13
	TraesCS5A02G092600	*TaPFK-A10*	420	6.50 / 45.752	Cy/Cp	13
	TraesCS5B02G098700	*TaPFK-B10*	412	6.12 / 44.926	Cy/Cp	13
	TraesCS5D02G104900	*TaPFK-D10*	420	6.36 / 45.718	Cy/Cp	13
PFP_ALPHA	TraesCS5A02G072700	*TaPFPα-A1*	621	6.83 / 67.597	Cy	19
	TraesCS5B02G078300	*TaPFPα-B1*	621	6.83 / 67.885	Cy	19
	TraesCS5D02G085500	*TaPFPα-D1*	621	6.85 / 67.692	Cy	19
	TraesCS6A02G279100	*TaPFPα-A2*	581	6.33 / 63.118	Cy	17
	TraesCS6B02G307200	*TaPFPα-B2*	616	6.76 / 67.059	Cy	17
	TraesCS6D02G259500	*TaPFPα-D2*	616	6.76 / 67.144	Cy	17
	TraesCS7A02G226000	*TaPFPα-A3*	611	6.27 / 66.818	Cy	18
	TraesCS7B02G193600	*TaPFPα-B3*	611	6.35 / 66.821	Cy	18
	TraesCS7D02G228500	*TaPFPα-D3*	611	6.35 / 66.853	Cy	18
PFP_BETA	TraesCS7A02G198200	*TaPFPβ-A*	560	5.83 / 60.558	Cy	16
	TraesCS7B02G104400	*TaPFPβ-B*	560	5.83 / 60.589	Cy	16
	TraesCS7D02G200800	*TaPFPβ-D*	560	5.83 / 60.558	Cy	16
cpFBP	TraesCS7A02G484200	*TacpFBP-A1*	391	8.27 / 42.406	Cp	3
	TraesCS7B02G387900	*TacpFBP-B1*	398	8.95 / 42.782	Cp	3
	TraesCS7D02G471600	*TacpFBP-D1*	397	8.57 / 42.764	Cp	3
	TraesCS4A02G093100	*TacpFBP-A2*	409	5.14 / 44.218	Cp	4
	TraesCS4B02G211400	*TacpFBP-B2*	409	5.07 / 44.276	Cp	4
	TraesCS4D02G212000	*TacpFBP-D2*	409	5.07 / 44.300	Cp	4
cyFBP	TraesCS3A02G377600	*TacyFBP-A1*	341	5.48 / 37.148	Cy	11
	TraesCS3B02G410400	*TacyFBP-B1*	341	5.38 / 37.206	Cy	11
	TraesCS3D02G370700	*TacyFBP-D1*	341	5.48 / 37.148	Cy	11
	TraesCS1A02G273900	*TacyFBP-A2*	341	5.70 / 37.113	Cy	10
	TraesCS1B02G283600	*TacyFBP-B2*	341	5.58 / 37.036	Cy	10
	TraesCS1D02G274000	*TacyFBP-D2.1*	341	5.87 / 37.067	Cy	10
	TraesCS1D02G274200	*TacyFBP-D2.2*	341	5.46 / 36.999	Cy	10

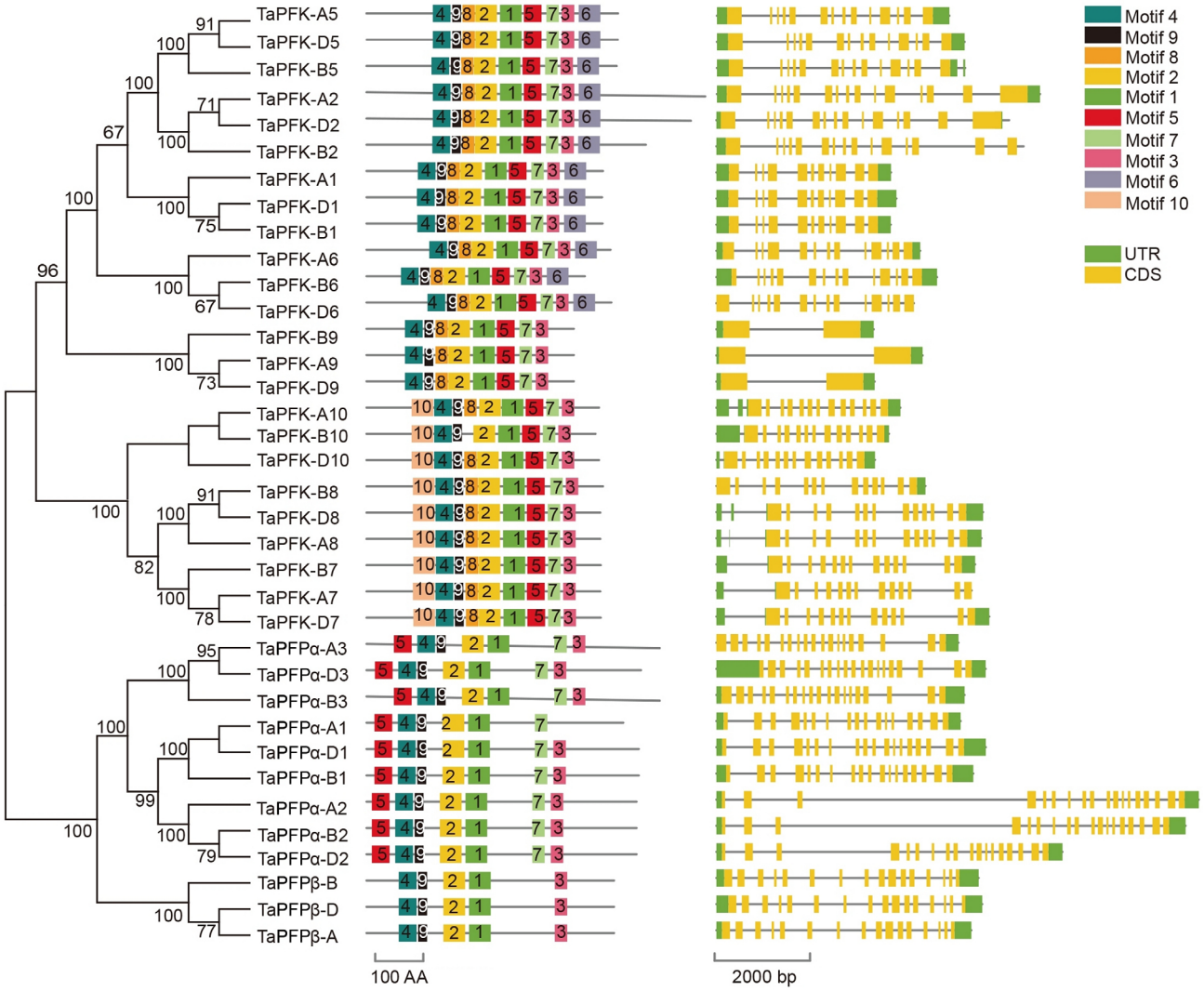

Fig. 1. Phylogenetic tree, conserved motifs, and gene structures of *TaPFK* and *PFP*. The tree was constructed by the neighbor-jointing method using amino acid sequences in *MEGA7.0*. Motifs and exons are indicated as *rectangles*, other sequences as *lines*. Motifs 1 - 4 and 9 are the F-6-P binding site, motif 8 is the ATP-binding site. CDS - coding sequence; PFK - ATP-dependent phosphofructokinase; PFP - pyrophosphate-dependent fructose-6-phosphate 1-phosphotransferase, Ta - *Triticum aestivum*; UTR - untranslated region.

three β isoforms in allohexaploid wheat interact with each other and regulate carbon efflux, remains to be elucidated.

Since signal peptides are present in the N-termini of cpFBPs, their peptide lengths are longer than those of cyFBPs (Table 1). All TaFBPs have nine conserved motifs (Fig. 2), except cpFBP1, which has an extra motif 9. We next aligned the TaFBPs to AtcyFBP (Fig. 4 Suppl.), which showed that substrate- or magnesium ion-binding sites are generally conserved in the FBP family. Compared to cpFBP1, cpFBP2 displayed some differences: two conserved motifs in the F-1,6-P_2-binding site, RYxG (AtcyFBP 246-249) and KLRL (AtcyFBP 277-280) were substituted by RYxC and HLRL, respectively. Moreover, a six-amino-acid deletion was found right before the KLRL conserved motif. Gutle *et al*. (2016), Serrato (2009), and Chueca *et al*. (2002) showed that these mutations (two amino acid substitutions and the deletion) are common in plant cpFBP2s (Fig. 4 Suppl.).

We assessed the expression of all members of the three gene families at different developmental stages of cv. CS. Fig. 3*A* shows that homoeologs of the same gene in the A, B, and D subgenome usually shared similar expression patterns. For example, *TaPFK-A1*, *B1*, and *D1* were more strongly expressed in the roots than in the stem. Of the eight *TaPFKs* (24 members in total), only *TaPFK-1* and *5* were highly expressed (more than 60 % of the total cytosol *TaPFKs*), whereas others were expressed at low levels or specifically in certain tissues. Among the three *PFPα*s, homoeologous *PFPα2*s were highly expressed in root, stem, and spikelet, but at relatively lower levels in leaves and developing grains. *PFPβ* expression patterns were very similar to those of *PFPα2*s (Fig. 3*A*). Among four *FBPs*, *cpFBP1*s and *cyFBP1s* were highly expressed in green tissues (80 - 150 transcripts per million, TPM), but rarely expressed in roots and developing grains (< 1 TPM). The expression of *cyFBP-D2.1* was lower than

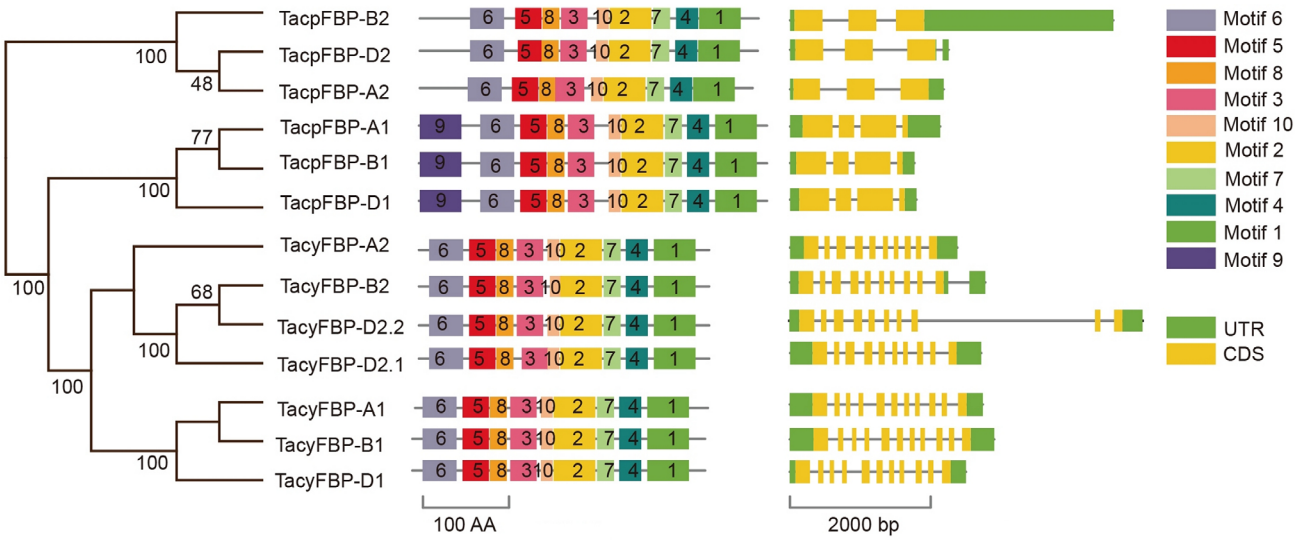

Fig. 2. Phylogenetic tree, conserved motifs, and gene structure of FBP. The tree was constructed by the neighbor-jointing method using amino acid sequences in *MEGA7.0*. Motifs and exons are indicated as *rectangles*, other sequences as *lines*. CDS - coding sequence; FBP - fructose-1,6-bisphosphatase; Ta - *Triticum aestivum*; UTR - untranslated region.

that of *cyFBP-D2.2*, and its expression pattern did not resemble that of *cyFBP-A2*, which is phylogenetically closely related (Fig. 2 and Fig. 3 Suppl.). Comparing all members of the three gene families, the expressions were as follows: *TacyFBP*-1s > *TacpFBP*-1s > *TaPFPα*-2s ≈ *TaPFPβs* >> *TaPFK*-1s ≈ *TaP*FK-5s >> the remaining genes in most of the tissues (Fig. 3*A*). Interestingly, in green tissues such as coleoptile, shoot, leaf blade, the number of total transcripts of *cyFBPs* and *cpFBPs* were higher (> 200 TPM) than those of *PFPα* and *PFPβ* (about 50~70 TPM), which was *vice versa* in sink tissue such as root, spikelets, and grain where *PFPα* and *PFPβ* were higher than that of *cyFBPs* and *cpFBPs*. Furthermore, in green tissues, *cyFBPs* were higher than *cpFBPs*. *PFKs* were relatively stable at different development stages (Fig. 3*B*). From the expression patterns, we concluded that products of photosynthesis (glyceraldehyde-3-phosphate and dihydroxyacetone phosphate) were actively converted to sucrose (in the cytoplasm) and starch (in the chloroplast) and that due to sucrose transport to sink tissues, the expression of *cyFBPs* was higher than that of *cpFBPs* in these tissues.

In summary, the highly expressed *PFKs*, *PFPs*, and *FBPs* in wheat were revealed through mining public RNA-Seq data. The expression of these members was more than 60 % of the total transcripts in most tissues (Fig. 3). As the RNA-Seq data have large sample numbers (Fig. 3), we believe these results may be close to the real situation *in vivo*. Furthermore, the regulation of gene activity could happen after translation (post-translational regulation). It was reported that pea cyFBP1 (*Pisum sativum*) is redox-regulated through thiol/disulfide switch (Serrato *et al.* 2018). Therefore, from the results inferred from *Arabidopsis*, rice, and this study (Lee *et al.* 2008, Rojas-Gonzalez *et al.* 2015, Soto-Suarez *et al.* 2016), future studies should target these main members to disclose their function in wheat not only at the transcriptional level.

The above results showed that *TaPFPs* are induced in sink tissue (Fig. 3*B*); to analyze *TaPFP* functions, we identified mutant lines in a fast neutron-induced mutant population of common wheat cv. HP3. A pair of conserved primers was used to detect mutations in all three *TaPFPβs* simultaneously (Table 1 Suppl.). We observed that the bands corresponding to *TaPFPβ-A*, *-B*, and *-D* were absent in the NT lines of CS (Fig. 4*A*), indicating that *TaPFPβ-A*, *-B*, and *-D* were located on chromosomes 7A, 7B, and 7D, respectively. The genotyping results showed that a few single plants lacked the band corresponding to *TaPFPβ-A*, whereas most plants harbored all three copies of *TaPFPβ* in line 686. In addition, we obtained a *TaPFPβ-B* mutant. Since we found only one heterozygote plant at the *TaPFPβ-D* locus in M2 plants, we further self-hybridized these plants to obtain a homozygous *βTaPFP-D* mutant in the M3 plants (data not shown). All mutant lines were further identified at the RNA level. Gene-specific primers were designed to detect the expression of *TaPFPβs*. As expected, *TaPFPβ-A*, *-B*, and *-D* transcripts were absent in lines 686 (or 419), 557, and 785 respectively (Fig. 4*B*). Thus, we obtained knockout mutant lines of all three *TaPFPβs*.

Based on field data collected over 2 years (2018 - 2019), we found that plant height and TGM of all mutant lines were decreased, especially in lines 668 (*tapfpβ-a*) and 557 (*tapfpβ-b*) (Fig. 5*A*,*B*), although all lines had normal grains. This phenotype is reminiscent of that of an *AtPFPβ* RNAi line with smaller rosette leaves (Lim *et al.* 2009). Since we could not establish *tapfpβ-a/b*, *tapfpβ-a/d*, and *tapfpβ-b/d* double-mutant lines by hybridization, we further observed the phenotype of anther and pollen (Fig. 5*C,D*, Fig. 5 Suppl.). Pollen grains of HP3 (WT) plants were round and well-developed, with only 4 % pale, collapsed, or irregularly shaped pollen (Fig. 5*C*, Fig. 5 Suppl., Fig. 6 Suppl.). However, in the mutant lines, especially, *tapfpβ-a* and *-d,* 12 - 13 % of the pollen grains

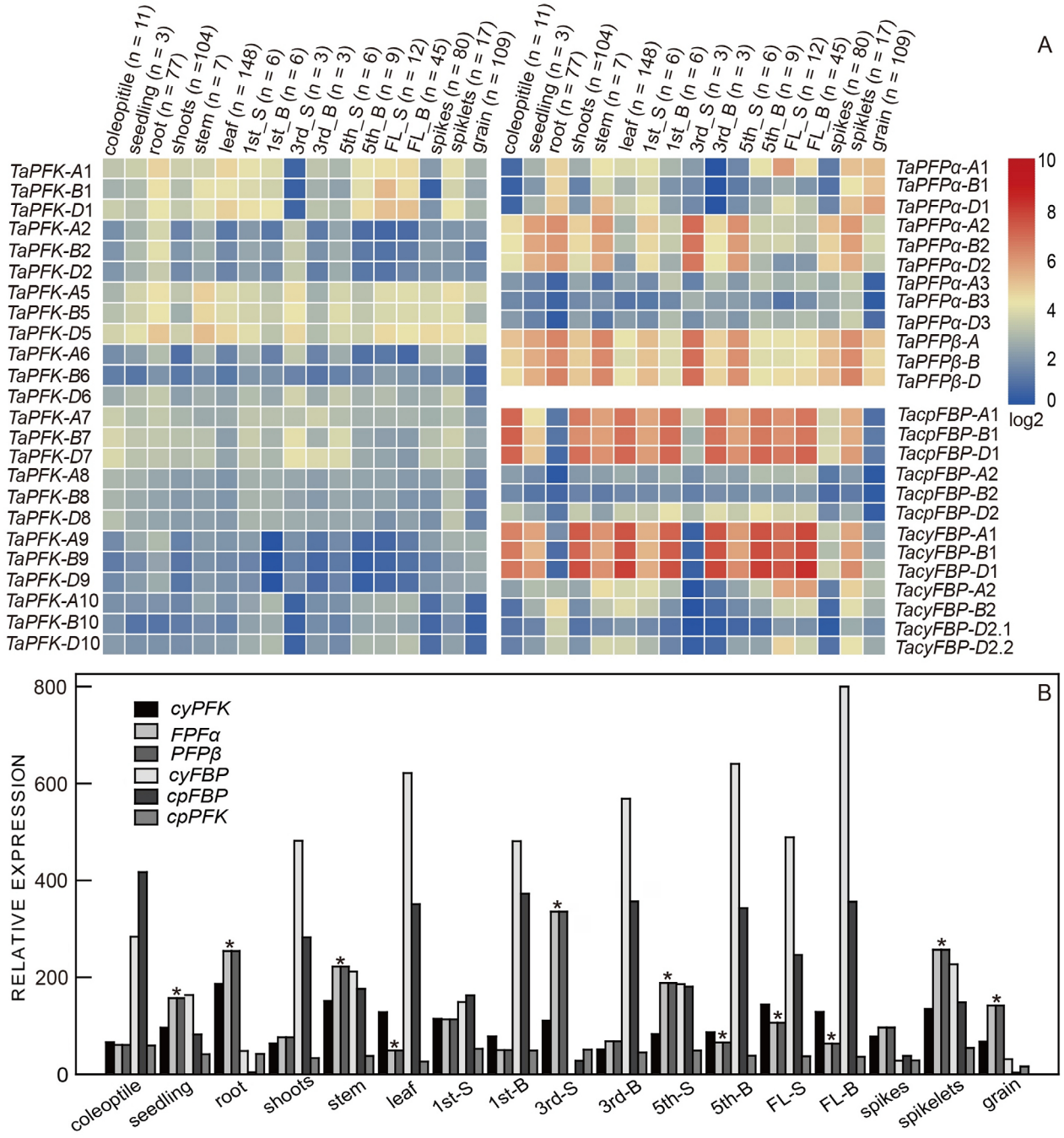

Fig. 3. Transcript profiling of *TaPFKs*, *TaPFPs*, and *TaFBPs* in different developmental stages of common wheat (CS). *A* - Heatmap of relative transcriptions of individual genes were shown by $\log_2$ TPM. *B* - Total amount of transcripts of different genes. *cyPFK* stands for the sum of *PFK*-1, -2, -5, -6, and -9 transcripts; *FPFα* - stands for *FPFα*-1, -2, and -3; *cyFBP* stands for *cyFBP-1* and *-2*; *cpFBP* stands for *cpFBP-1* and *-2; cpPFK* stands for *PFK-7, -8*, and *-10*; S - sheath; B - blade; FL - flag leaves; cy - cytoplasmic; cp - chloroplast; TPM - transcripts per million. Details of the genes were listed in Table 1. * indicated a significant difference at $P < 0.05$ (Student's *t*-test) between *PFP* and *PFKs;* n in Fig. 3*A* is the sample number.

showed abnormalities, including being stuck to each other (Fig. 5*C*, Fig. 5 Suppl. Fig. 6 Suppl.). These phenotypic findings may explain why we could not establish double or triple mutants. Thus, the lack of one copy of *TaPFPβ* decreased wheat vitality. Based on these findings, we concluded that the three homologs of *TaPFPβ* regulate plant growth additively in common wheat.

The hydrolysis of stored starch to glucose and the formation of ATP or other products through glycolysis and the TCA cycle are very important during seed germination (Fig. 1 Suppl.). Thus, we further observed the germination process in HP3 and *tapfpβ* mutant lines and found that, except for line 686 (*tapfpβ-a* mutant), which had a decreased germination rate, lengths of coleoptile, and

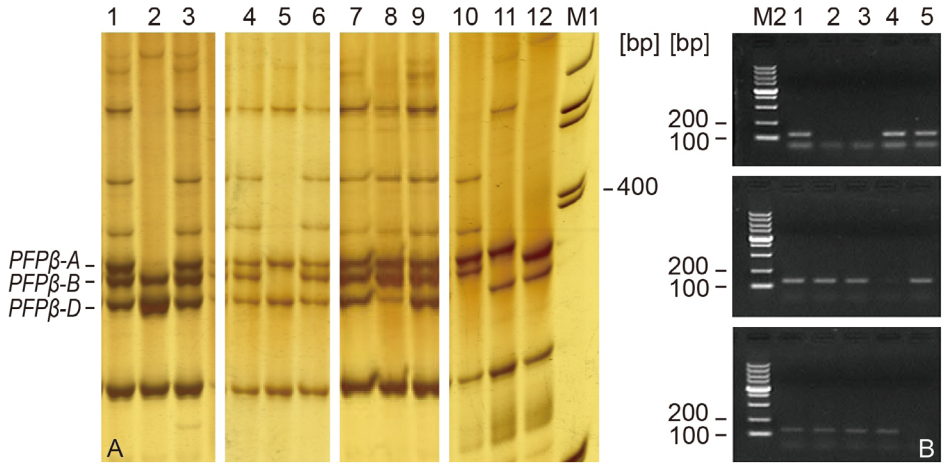

Fig. 4. Identification of *TaPFPβ* mutants in a neutron-induced mutant population of HP3. *A* - Genotyping of single plants. PCR products generated using conserved primers F1 and R1 (Table 1 Suppl.) and gDNA as a template were separated by 6 % PAGE. Lane 1 - 3, *pfpβ-a* mutant line 686 (data of line 419 was not shown); lane 4 - 6, *pfpβ-b* mutant line 557; lane 7 - 9, *pfpβ-d* mutant line 785; lane 10 - 12, CS null-tetrasomic lines N7DT7B, N7BT7A, and N7DT7B, respectively. *B* - Detection of RNA transcripts in the mutant lines. PCR products of *PFPβ-A* (upper panel), *PFPβ-B* (middle panel), and *PFPβ-D* (lower panel) generated using specific primers and cDNA as a template were separated by 1.5 % agarose gel electrophoresis. Lane 1, HP3; Mutant line of *pfpβ-a* (Lane 2, 3, line 419 and 686), *pfpβ-b* (Lane 4, line 557); and *pfpβ-d* (Lane 5, line 785). M1 - DNA marker 50 bp ladder; M2 - DL5000.

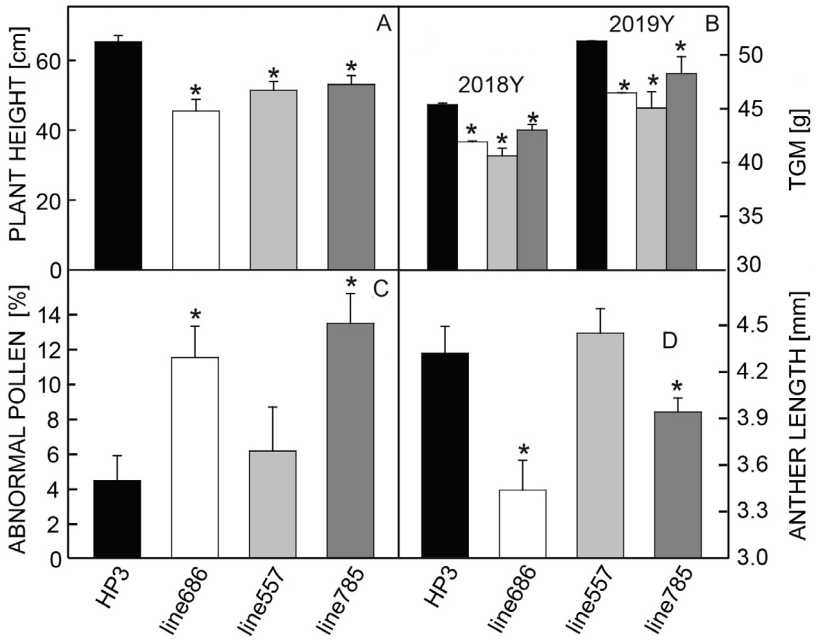

Fig. 5. Phenotypic analysis of *tapfpβ* mutant lines. *A* - Plant height of HP3 (WT) and three mutant lines, $n \geq 50$. *B* - Thousand-grain mass (TGM). Data were collected in 2018 and 2019, $n \geq 3$. *C* - Percentage of abnormal pollen grains in the four lines. *D* - Anther length.

primary root (Fig. 6*A* - *C*), other lines had no differences ($P < 0.05$). Fructose and glucose contents were slightly increased during germination in all lines (Fig. 6*D*,*E*) ($P < 0.05$). Sucrose content exhibited a decrease-increase-decrease dynamic trend during 24 - 96 h of germination (Fig. 6*F*). Interestingly, fructose contents were higher in all mutant lines than in the HP3 at 24 h, whereas the increase in fructose was relatively smaller in mutant lines at 24 - 72 h of germination. These findings indicated that fructose dynamics were affected by the loss of *TaPFPβ*. Moreover, in line 686 (*tapfpβ-a* mutant), fructose content was 2 - 3 times higher than those in other lines at the end of germination. A high fructose content may indicate that the metabolism downstream of fructose was hampered (Fig. 1 Suppl.). This would cause a shortage of ATP and other materials needed for DNA, RNA, and protein biosynthesis, which may have resulted in a lower germination rate or slower growth of young seedlings in line 686 than in the other lines (Fig. 6*A* - *C*).

To elucidate the mechanism underlying the differences in fructose content among the mutant lines and the HP3, we detected the expression of genes related to the F-6-P and F-1,6-P_2 balance. Gene-specific primers were designed based on the differences among the gene

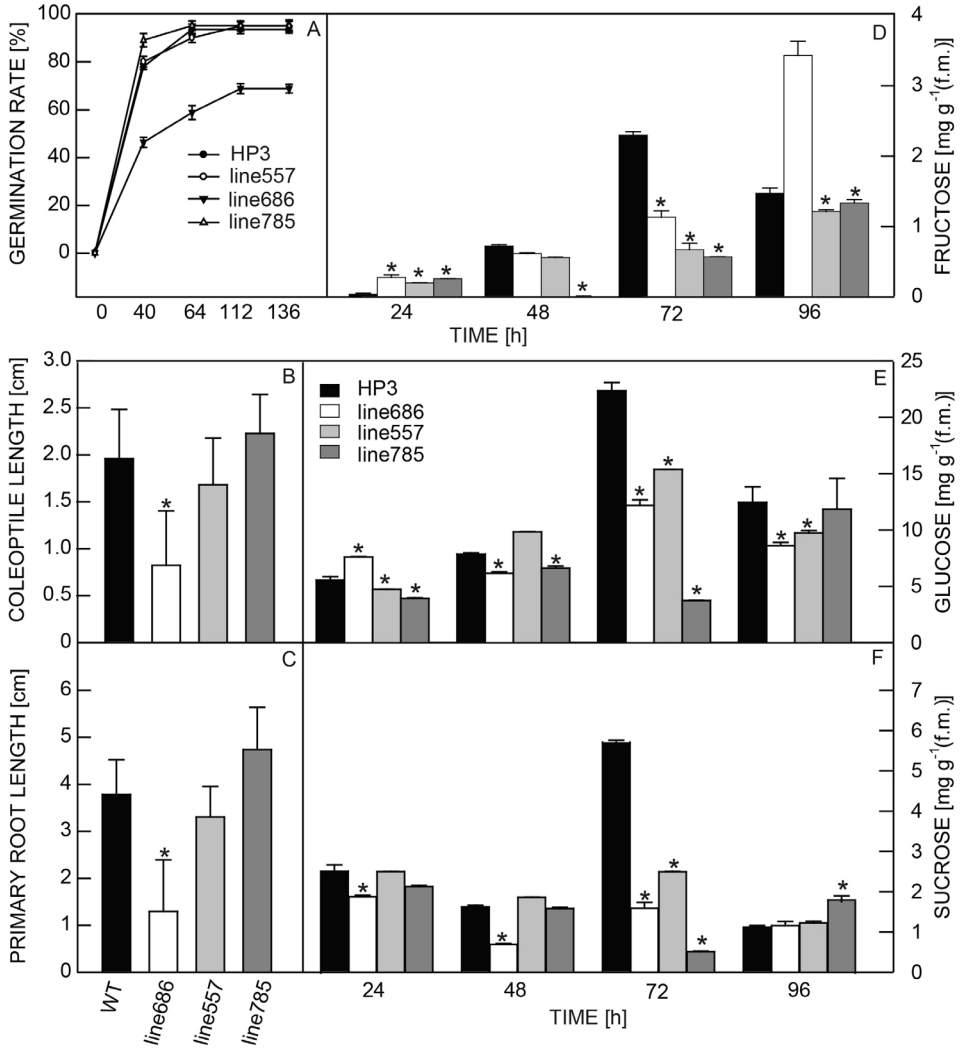

Fig. 6. Germination and soluble sugar content of *tapfpβ* mutant lines. *A* - Germination rate during 0 - 136 h; *B* - Length of coleoptile; *C* - Primary root length. All germination data were collected from at least three repeats and of 100 seeds. Means ± SDs. *D* - Fructose content; *E* - Glucose content; *F* - Sucrose content. Means ± SDs, $n \geq 3$ (biological and technical repeats), * - $P < 0.05$ (Student's *t*-test).

families (Table 1 Suppl.). The expression data revealed that: *1*) only a few members of *TaPFKs*, *TaPFPs*, and *TaFBPs* were expressed during germination; for example, homologous *TacyFBP*-1s were the only *TaFBPs* expressed during germination (Fig. 7); *2*) only *TaPFK*-5s and *TaPFP*α-2s were highly expressed in HP3, whereas the other genes were poorly expressed; *3*) in mutant lines, expressions of *TaPFK*-5s, *TaPFP*α-2s, and *TaPFPβs* were lower than those in the HP3; and *4*) fructose content was negatively correlated with expressions of total *TaPFPs* (R^2 = -0.6077~0.7787), but not with those of *TaPFKs* (Figs. 6*D* and 7). The negative relationship between *TaPFP* expression and fructose content was consistent with a previous finding, which showed that the downregulation of PFP activity in sugarcane elevated sucrose and hexose-phosphate content (Van der Merwe *et al.* 2010).

In higher plants, photosynthesis products are converted to sucrose and then transported to sink tissues (*e.g.* roots) or stored as starch (*e.g.*, in the grains) for further use. In the membranes of root cells, the abundant nitrogen, phosphorus, and mineral transporters consume large amounts of ATP (Léran *et al.* 2014). In developing spikelets and during seed germination, proteins, lipids, RNA, and DNA are very actively biosynthesized. In these tissues, stored sucrose or starches are metabolized through glycolysis and then shuttled to the tricarboxylic acid cycle to generate ATP and carbon skeletons for further biosynthesis; hence, the glycolysis pathway may prevail over the gluconeogenesis pathway in these tissues. To meet demands, organisms may upregulate the expression of enzymes in the glycolysis pathway. In contrast, in tissues such as leaves, sucrose and starch are stored for further use and thus, the glycolysis pathway may be downregulated to save energy. As shown in Fig. 3, transcriptions of *TaPFPα* and *PFPβ* were relatively higher in sink tissues such as the roots, spikelet, and grain, with transcript amounts of most *TaPFKs* lower in leaves than in roots or grains. During germination, *TaPFK-5* and *PFPα2* were more strongly expressed than *cyFBP*-1, indicating upregulation of the genes involved in the glycolysis pathway (Fig. 7).

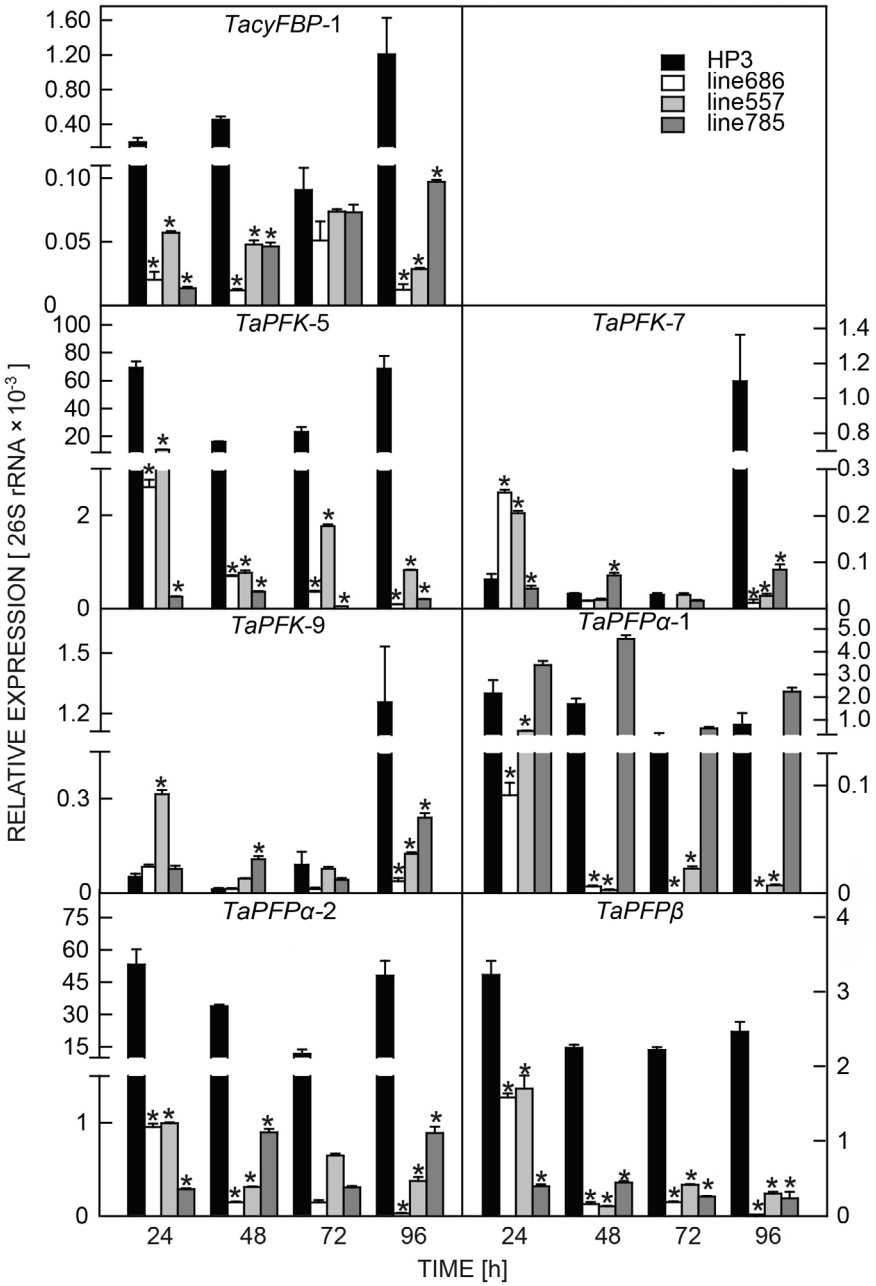

Fig. 7. Expression of *TaPFKs*, *TaPFP,* and *TaFBPs* during germination of WT and mutant lines. Transcriptions were detected after 24, 48, 72, and 96 h of germination. All transcriptions were normalized to *26S rRNA* gene expression. Means ± SDs (n = 3). * - $P < 0.05$ (Student's t-test).

Notably, F-2,6-P_2 is an activator of PFP, an inhibitor of FBP, but has no effect on ATP-PFK in plants (Muchut *et al.* 2019, Plaxton and Podestá 2007, Theodorou and Kruger 2001). F-2,6-P_2 content is consistently high in sink tissues but significantly varies in the leaf cytosol (Nielsen *et al.* 2004). This implies that high PFP activity is maintained in non-photosynthetic tissues. Nielsen and Stitt (2001) found that PFP expression and PFP enzyme activity at the base and tip of young growing leaves were decreased in tobacco. This validates our findings to a certain degree as the downregulation of *TaPFPβs* affected germination (or young seedling growth) and pollen development (Fig. 6, Figs 5 and 6 Suppl.). Based on the expression patterns, phenotypes of *tapfpβs* mutants, and previous findings, we conclude that TaPFP is essential in sink tissues.

Conclusions

In this study, we identified three gene families namely *TaPFK*, *TaPFP*, and *TaFBP*, which are involved in the balance between F-6-P and F-1,6-P_2. From the phylogenic analysis, we found that gene loss and duplication occurred at different time points during grass genome evolution and shaped the gene variability in the three gene families in grass species. Based on expression profiling of these genes and phenotypic analyses (at the morphological, cellular, and physiological levels) of *tapfpβ* mutant lines, we found that TaPFP functions dominate those of TaPFKs during seed germination, seedling growth, and pollen grain development in wheat. For further studies, modern *CRISPR/Cas* technology should be used to obtain homologous *TaPFK*- and *TaFBP*-knockout lines (main expressed members) and to unravel how these genes are involved in wheat development and yield production.

References

Ali-Benali, M.A., Alary, R., Joudrier, P., Gautier, M.F.: Comparative expression of five *Lea* genes during wheat seed development and in response to abiotic stresses by real-time quantitative RT-PCR. - Biochim. biophys. Acta **1730**: 56-65, 2005.

Ap Rees, T., Green, J.H., Wilson P.M.: Pyrophosphate: fructose 6-phosphate 1-phosphotransferase and glycolysis in non-photosynthetic tissues of higher plants. - Biochem. J. **227**: 299-304, 1985.

Basson, C.E., Groenewald, J.H., Kossmann, J., Cronje, C., Bauer R.: Upregulation of pyrophosphate: fructose 6-phosphate 1-phosphotransferase (PFP) activity in strawberry. - Transgenic Res. **20**: 925-931, 2011.

Borrill, P., Ramirez-Gonzalez, R., Uauy, C.: expVIP: a customizable RNA-seq data analysis and visualization platform. - Plant Physiol. **170**: 2172-2186, 2016.

Brenchley, R., Spannagl, M., Pfeifer, M., Barker, G.L., D'Amore, R., Allen, A.M., McKenzie, N., Kramer, M., Kerhornou, A., Bolser, D., Kay, S., Waite, D., Trick, M., Bancroft, I., Gu. Y., Huo, N., Luo, M.C., Sehgal, S., Gill, B., Kianian, S., Anderson, O., Kersey, P., Dvorak, J., McCombie, W.R., Hall, A., Mayer, K.F., Edwards, K.J., Bevan, M.W., Hall N.: Analysis of the bread wheat genome using whole-genome shotgun sequencing. - Nature **491**: 705-710, 2012.

Cao, J., Dai, X., Wang Q. (ed.): Botanical Experiment. - China Sci. Publishing & Midia Ltd., Beijing, 2012. [In Chinese]

Chen, C., He, B., Liu, X., Ma, X., Liu, Y., Yao, H.Y., Zhang, P., Yin, J., Wei, X., Koh, H.J., Yang, C., Xue, H.W., Fang, Z., Qiao, Y.: Pyrophosphate-fructose 6-phosphate 1-phosphotransferase (PFP1) regulates starch biosynthesis and seed development *via* heterotetramer formation in rice (*Oryza sativa* L.). - Plant Biotechnol. J. **18**: 83-95, 2020a.

Chen, C., Chen, H., Zhang, Y., Thomas, H.R., Frank, M.H., He, Y., Xia, R.: TBtools: An integrative toolkit developed for interactive analyses of big biological data. - Mol. Plant **13**: 1194-1202, 2020b.

Chueca, A., Sahrawy, M., Pagano, E.A., Lopez Gorge, J.: Chloroplast fructose-1,6-bisphosphatase: structure and function. - Photosynth. Res. **74**: 235-249, 2002.

Costa dos Santos, A., Seixas da-Silva, W., De Meis, L., Galina, A.: Proton transport in maize tonoplasts supported by fructose-1,6-bisphosphate cleavage. Pyrophosphate-dependent phosphofructokinase as a pyrophosphate-regenerating system. - Plant Physiol. **133**: 885-892, 2003.

Duan, E., Wang, Y., Liu, L., Zhu, J., Zhong, M., Zhang, H., Li, S., Ding, B., Zhang, X., Guo, X., Jiang, L., Wan, J. Pyrophosphate: fructose-6-phosphate 1-phosphotransferase (PFP) regulates carbon metabolism during grain filling in rice. - Plant Cell Rep. **35**: 1321-1331, 2016.

Fernie, A.R., Roscher, A., Ratcliffe, R.G., Kruger, N.J.: Fructose 2,6-bisphosphate activates pyrophosphate: fructose-6-phosphate 1-phosphotransferase and increases triose phosphate to hexose phosphate cycling in heterotrophic cells. - Planta **212**: 250-263, 2001.

Fernie, A.R., Roscher, A., Ratcliffe, R.G., Kruger, N.J.: Activation of pyrophosphate: fructose-6-phosphate 1-phosphotransferase by fructose 2,6-bisphosphate stimulates conversion of hexose phosphates to triose phosphates but does not influence accumulation of carbohydrates in phosphate-deficient tobacco cells. - Physiol. Plant. **114**: 172-181, 2002.

Fernie, A.R., Carrari, F., Sweetlove, L.J.: Respiratory metabolism: glycolysis, the TCA cycle and mitochondrial electron transport. - Curr. Opin. Plant Biol. **7**: 254-261, 2004.

Gutle, D.D., Roret, T., Muller, S.J., Couturier, J., Lemaire, S.D., Hecker, A., Dhalleine, T., Buchanan, B.B., Reski, R., Einsle, O., Jacquot, J.P.: Chloroplast FBPase and SBPase are thioredoxin-linked enzymes with similar architecture but different evolutionary histories. - Proc. nat. Acad. Sci. USA **113**: 6779-6784, 2016.

International Wheat Genome Sequencing C.: A chromosome-based draft sequence of the hexaploid bread wheat (*Triticum aestivum*) genome. - Science **345**: 1251788, 2014.

International Wheat Genome Sequencing C.: Shifting the limits in wheat research and breeding using a fully annotated reference genome. - Science **361**: eaar7191, 2018.

Jia, J., Zhao, S., Kong, X., Li, Y., Zhao, G., He, W., Appels, R., Pfeifer, M., Tao, Y., Zhang, X., Jing, R., Zhang, C., Ma, Y., Gao, L., Gao, C., Spannagl, M., Mayer, K.F., Li, D., Pan, S., Zheng, F., Hu, Q., Xia, X., Li, J., Liang, Q., Chen, J., Wicker, T., Gou, C., Kuang, H., He, G., Luo, Y., Keller, B., Xia, Q., Lu, P., Wang, J., Zou, H., Zhang, R., Xu, J., Gao, J., Middleton, C., Quan, Z., Liu, G., Wang, J., Yang, H., Liu, X., He, Z., Mao, L., Wang, J.: *Aegilops tauschii* draft genome sequence reveals a gene repertoire for wheat adaptation. - Nature **496**: 91-95, 2013.

Jiang, Y.H., Wang, D.Y., Wen, J.F.: The independent prokaryotic origins of eukaryotic fructose-1, 6-bisphosphatase and sedoheptulose-1, 7-bisphosphatase and the implications of their origins for the evolution of eukaryotic Calvin cycle. - BMC Evol. Biol. **12**: 208, 2012.

Knowles, V.L., Greyson, M.F., Dennis, D.T.: Characterization of ATP-dependent fructose 6-phosphate 1-phosphotransferase isozymes from leaf and endosperm tissues of *Ricinus communis*. - Plant Physiol. **92**: 155-159, 1990.

Kumar, S., Stecher, G., Tamura, K.: MEGA7: molecular evolutionary genetics analysis version 7.0 for bigger datasets. - Mol. Biol. Evol. **33**: 1870-1874, 2016.

Lee, S.K., Jeon, J.S., Bornke, F., Voll, L., Cho, J.I., Goh, C.H., Jeong, S.W., Park, Y.I., Kim, S.J., Choi, S.B., Miyao, A., Hirochika, H., An, G., Cho, M.H., Bhoo, S.H., Sonnewald, U., Hahn, T.R.: Loss of cytosolic fructose-1,6-bisphosphatase limits photosynthetic sucrose synthesis and causes severe growth retardations in rice (*Oryza sativa*). - Plant Cell Environ. **31**: 1851-1863, 2008.

Léran, S., Varala, K.K., Boyer, J.C., Chiurazzi, M., Crawford, N., Daniel-Vedele, F., David, L., Dickstein, R., Fernandez, E., Forde, B., Gassmann, W., Geiger, D., Gojon, A., Gong, J.M., Halkier, B.A., Harris, J.M., Hedrich, R., Limami,

A.M., Rentsch, D., Seo, M., Tsay, Y.F., Zhang, M., Coruzzi, G., Lacombe, B.: A unified nomenclature of NITRATE TRANSPORTER 1/PEPTIDE TRANSPORTER family members in plants. - Trends Plant Sci. **19**: 5-9, 2014.

Lim, H., Cho, M.H., Bhoo, S.H., Hahn, T.R.: Pyrophosphate: fructose-6-phosphate 1-phosphotransferase is involved in the tolerance of *Arabidopsis* seedlings to salt and osmotic stresses. - *In Vitro* Cell. Dev. Plant **50**: 84-91, 2013.

Lim, H., Cho, M.H., Jeon, J.S., Bhoo, S.H., Kwon, Y.K., Hahn, T.R.: Altered expression of pyrophosphate: fructose-6-phosphate 1-phosphotransferase affects the growth of transgenic *Arabidopsis* plants. - Mol. Cells **27**: 641-649, 2009.

Ling, H.Q., Zhao, S., Liu, D., Wang, J., Sun, H., Zhang, C., Fan, H., Li, D., Dong, L., Tao, Y., Gao, C., Wu, H., Li, Y., Cui, Y., Guo, X., Zheng, S., Wang, B., Yu, K., Liang, Q., Yang, W., Lou, X., Chen, J., Feng, M., Jian, J., Zhang, X., Luo, G., Jiang, Y., Liu, J., Wang, Z., Sha, Y., Zhang, B., Wu, H., Tang, D., Shen, Q., Xue, P., Zou, S., Wang, X., Liu, X., Wang, F., Yang, Y., An, X., Dong, Z., Zhang, K., Zhang, X., Luo, M.C., Dvorak, J., Tong, Y., Wang, J., Yang, H., Li, Z., Wang, D., Zhang, A., Wang, J.: Draft genome of the wheat A-genome progenitor *Triticum urartu*. - Nature **496**: 87-90, 2013.

Lü, H., Li, J., Huang, Y., Zhang, M., Zhang, S., Wu, J.: Genome-wide identification, expression and functional analysis of the phosphofructokinase gene family in Chinese white pear (*Pyrus bretschneideri*). - Gene **702**: 133-142, 2019.

Marcussen, T., Sandve, S.R., Heier, L., Spannagl, M., Pfeifer, M., Jakobsen, K.S., Wulff, B.B., Steuernagel, B., Mayer, K.F., Olsen, O.A.: Ancient hybridizations among the ancestral genomes of bread wheat. - Science **345**: 1250092, 2014.

Martin, W., Mustafa, A.Z., Henze, K., Schnarrenberger, C.: Higher-plant chloroplast and cytosolic fructose-1,6-bisphosphatase isoenzymes: origins *via* duplication rather than prokaryote-eukaryote divergence. - Plant mol. Biol. **32**: 485-491, 1996.

Merril, C.R.: Silver staining of proteins and DNA. - Nature **343**: 779-780, 1990.

Mirzaghaderi, G., Mason, A.S.: Revisiting pivotal-differential genome evolution in wheat. - Trends Plant Sci. **22**: 674-684, 2017.

Montavon, P., Kruger, N.J.: Substrate specificity of pyrophosphate:fructose 6-phosphate 1-phosphotransferase from potato tuber. - Plant Physiol. **99**: 1487-1492, 1992.

Muchut, R.J., Piattoni, C.V., Margarit, E., Tripodi, K.E.J., Podesta, F.E., Iglesias, A.A.: Heterologous expression and kinetic characterization of the alpha, beta and alpha beta blend of the PPi-dependent phosphofructokinase from *Citrus sinensis*. - Plant Sci. **280**: 348-354, 2019.

Mustroph, A., Sonnewald, U., Biemelt, S.: Characterisation of the ATP-dependent phosphofructokinase gene family from *Arabidopsis thaliana*. - FEBS Lett. **581**: 2401-2410, 2007.

Mustroph, A., Stock, J., Hess, N., Aldous, S., Dreilich, A., Grimm, B.: Characterization of the phosphofructokinase gene family in rice and its expression under oxygen deficiency stress. - Front. Plant Sci. **4**: 125, 2013.

Nielsen, T.H., Stitt, S.M.: Tobacco transformants with strongly decreased expression of pyrophosphate:fructose-6-phosphate expression in the base of their young growing leaves contain much higher levels of fructose-2,6-bisphosphate but no major changes in fluxes. - Planta **214**: 106-116, 2001.

Nielsen, T.H., Rung, J.H., Villadsen, D.: Fructose-2,6-bisphosphate: a traffic signal in plant metabolism. - Trends Plant Sci. **9**: 556-563, 2004.

Noggle, G.R., Zill, L.P.: The quantitative analysis of sugars in plant extracts by ion-exchange chromatography. - Arch. Biochem. Biophys. **41**: 21-28, 1952.

Pfister, B., Zeeman, S.C.: Formation of starch in plant cells. - Cell Mol. Life Sci. **73**: 2781-2807, 2016.

Plaxton, W.C., Podestá, F.E.: The functional organization and control of plant respiration. - Crit. Rev. Plant Sci. **25**: 159-198, 2007.

Rojas-Gonzalez, J.A., Soto-Suarez, M., Garcia-Diaz, A., Romero-Puertas, M.C., Sandalio, L.M., Merida, A., Thormahlen, I., Geigenberger, P., Serrato, A.J., Sahrawy, M.: Disruption of both chloroplastic and cytosolic FBPase genes results in a dwarf phenotype and important starch and metabolite changes in *Arabidopsis thaliana*. - J. exp. Bot. **66**: 2673-2689, 2015.

Ronimus, R.S., Morgan, H.W.: The biochemical properties and phylogenies of phosphofructokinases from extremophiles. - Extremophiles **5**: 357-373, 2001.

Saitou, N., Nei, M.: The neighbor-joining method: a new method for reconstructing phylogenetic trees. - Mol. Biol. Evol. **4**: 406-425, 1987.

Salse, J., Bolot, S., Throude, M., Jouffe, V., Piegu, B., Quraishi, U.M., Calcagno, T., Cooke, R., Delseny, M., Feuillet, C.: Identification and characterization of shared duplications between rice and wheat provide new insight into grass genome evolution. - Plant Cell **20**: 11-24, 2008.

Senapati, N., Semenov, M.A.: Large genetic yield potential and genetic yield gap estimated for wheat in Europe. - Global Food Secur. **24**: 100340, 2020.

Serrato, A.J., Yubero-Serrano, E.M., Sandalio, L.M., Munoz-Blanco, J., Chueca, A., Caballero, J.L., Sahrawy, M.: cpFBPaseII, a novel redox-independent chloroplastic isoform of fructose-1,6-bisphosphatase. - Plant Cell Environ. **32**: 811-827, 2009.

Serrato, A.J., Romero-Puertas, M.C., Lázaro-Payo, A., Sahrawy, M.: Regulation by S-nitrosylation of the Calvin-Benson cycle fructose-1,6-bisphosphatase in *Pisum sativum*. - Redox Biol. **14**: 409-416, 2018.

Shew, A.M., Tack, J.B., Nalley, L.L., Chaminuka, P.: Yield reduction under climate warming varies among wheat cultivars in South Africa. - Nat. Commun. **11**: 4408, 2020.

Soto-Suarez, M., Serrato, A.J., Rojas-Gonzalez, J.A., Bautista, R., Sahrawy, M.: Transcriptomic and proteomic approach to identify differentially expressed genes and proteins in *Arabidopsis thaliana* mutants lacking chloroplastic 1 and cytosolic FBPases reveals several levels of metabolic regulation. - BMC Plant Biol. **16**: 258, 2016.

Theodorou, M.E., Kruger, N.J.: Physiological relevance of fructose 2,6-bisphosphate in the regulation of spinach leaf pyrophosphate:fructose 6-phosphate 1-phosphotransferase. - Planta **213**: 147-157, 2001.

Theodorou, M.E., Plaxton, W.C.: Purification and characterization of pyrophosphate-dependent phosphofructokinase from phosphate-starved *Brassica nigra* suspension cells. - Plant Physiol. **112**: 343-351, 1996.

Tripodi, K., Podesta, F.E.: Purification and structural and kinetic characterization of the pyrophosphate: fructose-6-phosphate 1-phosphotransferase from the Crassulacean acid metabolism plant, pineapple. - Plant Physiol. **113**: 779-786, 1997.

Turner, W.L., Plaxton, W.C.: Purification and characterization of pyrophosphate- and ATP-dependent phosphofructokinases from banana fruit. - Planta **217**: 113-121, 2003.

Van der Merwe, M.J., Groenewald, J.H., Stitt, M., Kossmann, J., Botha, F.C.: Downregulation of pyrophosphate: D-fructose-6-phosphate 1-phosphotransferase activity in sugarcane culms enhances sucrose accumulation due to elevated hexose-phosphate levels. - Planta **231**: 595-608, 2010.

Wang, P., Moore, B.M., Panchy, N.L., Meng, F., Lehti-Shiu, M.D., Shiu S.H.: Factors influencing gene family size variation among related species in a plant family, *Solanaceae*.

- Genome Biol. Evol. **10**: 2596-2613, 2018.
Winkler, C., Delvos, B., Martin, W., Henze, K.: Purification, microsequencing and cloning of spinach ATP-dependent phosphofructokinase link sequence and function for the plant enzyme. - FEBS J. **274**: 429-438, 2007.
Zhu, L., Zhang, J., Chen, Y., Pan, H., Ming, R.: Identification and genes expression analysis of ATP-dependent phosphofructokinase family members among three *Saccharum* species. - Funct. Plant Biol. **40**: 369, 2013.